Bull Volcanol (1986) 48: 109–125

Bulletin of
Volcanology

Quantitative models of the fallout and dispersal of tephra from volcanic eruption columns

S Carey[1] and RSJ Sparks[2]

[1] Graduate School of Oceanography, University of Rhode Island, Kingston, RI 02881, USA
[2] Department of Earth Sciences, University of Cambridge, Cambridge CB2 3EQ, UK

Abstract. A theoretical model of clast fallout from convective eruption columns has been developed which quantifies how the maximum clast size dispersal is determined by column height and wind strength. An eruption column consists of a buoyant convecting region which rises to a height H_B where the column density equals that of the atmosphere. Above H_B the column rises further to a height H_T due to excess momentum. Between H_T and H_B the column is forced laterally into the atmosphere to form an upper umbrella region. Within the eruption column, the vertical and horizontal velocity fields can be calculated from exprimental and theoretical studies and consideration of mass continuity. The centreline vertical velocity falls as a nearly linear function over most of the column's height and the velocity decreases as a gaussian function radially away from the centreline. Both column height and vertical velocity are strong functions of magma discharge rate. From calculations of the velocity field and the terminal fall velocity of clasts, a series of particle support envelopes has been constructed which represents positions where the column vertical velocity and terminal velocity are equal for a clast of specific size and density. The maximum range of a clast is determined in the absence of wind by the maximum width of the clast support envelope.

The trajectories of clasts leaving their relevant support envelope at its maximum width have been modelled in columns from 6 to 43 km high with no wind and in a wind field. From these calculations the shapes and areas of maximum grain size contours of the air-fall deposit have been predicted. For the no wind case the theoretical isopleths show good agreement with the Fogo A plinian deposit in the Azores. A diagram has been constructed which plots, for a particular clast size, the maximum range normal to the dispersal axis against the downward range. From the diagram the column height (and hence magma discharge rate) and wind velocity can be determined. Historic plinian eruptions of Santa Maria (1902) and Mount St. Helens (1980) give maximum heights of 34 and 19 km respectively and maximum wind speeds at the tropopause of 14 m/s and 30 m/s respectively. Both estimates are in good agreement with observations. The model has been applied to a number of other plinian deposits, including the ultraplinian phase of the *A.D.* 180 Taupo eruption in New Zealand which had an estimated column height of 51 km and wind velocity of 27 m/s.

Offprint requests to: S Carey

Introduction

The grain size charactistics and dispersal patterns of pyroclastic fall deposits formed from magmatic eruptions are known to be controlled principally by the height of the eruption column and the strength and direction of the wind (Eaton 1963; Walker 1973, 1981). Although substantial amounts of data have now been gathered concerning the grain size variations of fall deposits, inferences on the dimensions of the eruption columns and on the wind conditions have been largely qualitative. The most fundamental problem in interpreting fall deposits concerns distinguishing between the influence of the column and the wind on grain size and dispersal. A given grain size distribution at a local site could represent either a relatively low column height and strong wind or a relatively high column and weak wind. So far, attempts on modelling fallout patterns have been unable to remove the ambiguity. Models either assume some kind of average wind conditions (Shaw et al. 1974) or involve modelling fallout of historic eruptions where the wind strength is known (Carey and Sigurdsson 1982; Brazier et al. 1982).

Progress has been inhibited by the incomplete understanding of the dynamics of volcanic eruption columns and their interaction with wind. Some aspects of the problem have, however, been successfully tackled. The terminal fall velocities of pyroclasts are known from theoretical and experimental studies over a wide range of clast dimensions, shapes and densities (Walker et al. 1971; Wilson and Huang

1979). The ballistic trajectories of large clasts from volcanic explosions have been calculated (Wilson 1972, 1980). These calculations, however, only apply to the largest clasts with terminal velocities which are sufficiently great to avoid entrainment into the eruption column and which are also little affected by the wind. Ballistic clasts yield important information on gas exit velocities and explosion pressures (Wilson 1976, 1980; Wilson et al. 1980) but not on column heights and eruption intensities. The majority of early fallout models failed to treat the vertical gradation in pyroclast size which must occur within an eruption column. A common assumption involves instantaneous injection of a thoroughly mixed gas/particle cloud which then disperses by diffusion and lateral wind transport (Knox and Short 1964; Slaughter and Hamil 1970; Shaw et al. 1974; Allen 1982). This type of treatment stems, to some extent, from analogies with thermonuclear explosions and may have limited application to certain types of "instantaneous" explosive eruptions, such as vulcanian events. For the modelling of distal fallout of ash-sized pyroclasts, assumptions concerning the finer details of the source column are less critical yet become significant when proximal fall deposits are considered. A recent model by Suzuki (1983) improves the treatment of proximal deposition by incorporating a radially expanding column with a continuously decaying vertical velocity component, but is not based on a rigorous model of convectively-rising plumes.

Recent progress has been made on developing a more quantitative understanding of sustained convective eruption columns. Wilson et al. (1978), Settle (1978) and Fedotov (1985) have demonstrated that theories for the behaviour of simple thermal plumes could be adapted to eruption columns despite a number of complicating factors. They showed that the total height of a convecting eruption column is proportional to the fourth root of the mass discharge rate of magma (a measure of the eruption intensity). Subsequent studies of recent events, such as the 1979 eruption of Soufriere, St. Vincent, the 1980 eruption of Mount St. Helens, and the 1982 eruptions of El Chichon have corroborated this relationship (Sparks and Wilson 1982; Carey and Sigurdsson 1985, 1986). Sparks and Wilson (1982) also showed that thermal plume theory could be successfully adapted to estimate the variations of velocity and column width with height. Sparks (1986) presented some numerical calculations, which add some refinements to the earlier models based on modification of thermal plume theory (Morton et al. 1956; Turner 1979). The influence of magma temperature, the temperature inversion at the tropopause, height of the tropopause and the decrease in hydrostatic pressure with altitude on column dynamics were considered. Sparks estimated that, due to the expansion of air with height, eruption columns will spread faster than thermal plumes on a laboratory scale, with the discrepancy becoming substantial for very big columns. Behaviour is only weakly dependent on climatic factors.

An important phenomenon related to the bevaviour of sustained eruption columns has been highlighted by data obtained from satellites on the giant eruption cloud of Mount St. Helens on May 18, 1980 (Rice 1981; Sparks et al. 1986). A few minutes after the eruption began, a giant cloud ascended from the Mount St. Helens area to an altitude of 25 km. The cloud spread out laterally between 15 and 25 km to form an umbrella shaped cloud which expanded over 10 km upwind and reached a stagnation point where the stratospheric wind velocity and the radial expansion velocity were equal to each other. The radial expansion illustrated that, in eruptions with large mass discharge rates, the dynamic motions in the uppermost parts of the column could have a great effect on the shape and behaviour of a column. The event also gave an opportunity to observe how very large eruption clouds are affected by the wind. Sparks (1986) considered the radial expansion of the upper umbrella shaped region of an eruption column and found that a simple model based on continuity of mass flow rates produces results which agree well with the Mount St. Helens data. The significance of these ideas and observation in the present context is that the radial expansion of the upper regions of a large eruption column will have an important influence on the fallout and dispersal of ejecta.

This paper utilizes the theoretical and empirical information on column behaviour to develop a general model of ejecta fallout in near-vent regions. The case of columns in the absence of any wind is first examined. The isopleths of support for fragments of different size and density are calculated within eruption columns from 7-43 km high. The isopleth contours represent the points where statistically, the terminal fall velocity of the clast equals the vertical velocity of the column. The trajectories of clasts in the radially expanding upper part of the column are determined to give the *maximum range* of each clast size. The results are compared with data from the Fogo A deposit of Sao Miguel in the Azores, which is a rare example of a major plinian event where there was negligible wind (Walker and Croasdale 1971).

Some theoretical and empirical ideas on how eruption columns might be affected by the wind are presented. The downwind, crosswind and upwind ranges of maximum clast size are calculated and compared with the results of the wind-absent case. The models allow discrimination between the influence of column height and wind strength. The models are used to assess conditions during some well-documented eruptions, including some historic examples where the validity of the models can be tested.

Clast transport in eruption columns

Figure 1 depicts the main features of an eruption column. The physics of columns has been discussed elsewhere (Wil-

son 1976; Sparks 1986) and only the features relevant to the transport of clasts are summarized here. The base of the column is the momentum-dominated gas thrust region where velocities are high (hundreds of m/s) and decelerations large. In the lower region of the column the largest clasts are initially accelerated by the gas and then pursue ballistic trajectories which are influenced only weakly by the motion of decelerating gases around them. Ballistic clasts can leave the column altogether if their angle of ejection with respect to the vertical column axis is large enough. The range of such clasts is determined by their initial velocity, ejection angle, size and density (Wilson 1972). Such ballistic clasts can yield no information on the column height and eruption intensity. Their behaviour is determined by processes at the very base of the column.

The convective region of a column is where buoyancy forces dominate; it typically occupies most of the column's height. Although the velocities are smaller than the initial exit velocities they can still be tens to over 200 m/s. The column velocity decreases steadily with height. Models and observational data (Sparks 1986) suggest that over much of a column's height the mean velocity on the central axis decreases in an approximately linear fashion with height. Significant departure from a linear decrease only occurs at the bottom and top of a column. The convective velocities at a given height also increase systematically with magma discharge rate and thus with total column height. Sparks (1986) gives quantitative expressions of these relationships.

A convective eruption column is highly turbulent and thus local velocities at any position will fluctuate irregularly and substantially with time. However, studies of thermal plumes (Rouse et al. 1952; Turner 1979) show that the time-averaged vertical velocity U_v is a symmetrical gaussian function of distance from the plume axis:

$$U_v = U_c e^{-x^2/b^2}, \quad (1)$$

where U_c is the centreline velocity at height h, x is the radial distance and b is the distance at which the velocity has decreased to 1/e times U_c. Sparks and Wilson (1982) found that the *visible* edge of a volcanic plume corresponds approximately to a radius of $2b$.

The convective velocities within columns are sufficiently large that, in most situations, most ejecta will be carried up to the top of the convecting region. Some clasts will be carried to the column edge where vertical velocities are small and fallout will occur (Fig. 1). However, except in the weakest eruptions, the centreline convective velocities are great enough to carry some fist-sized clasts (5 cm lithics) to near the top of the column. Most clasts are entrained in the ascending column and do *not* follow ballistic trajectories. Only the very largest clasts (tens of centimeters) follow truly ballistic paths.

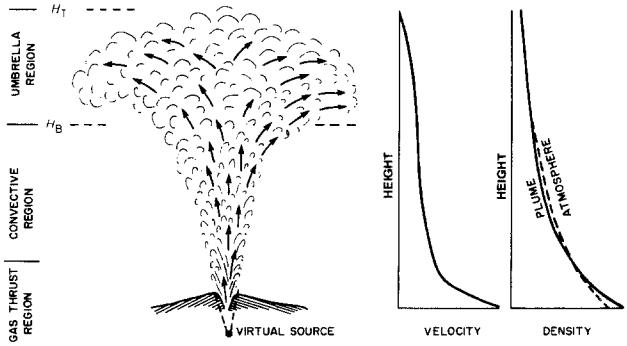

Fig. 1. Sketch of the main features of a convecting eruption column. Variation of centreline velocity and density with height are schematically shown

The uppermost part of a column is characterized by intrusion laterally into the atmosphere (Fig. 1) to form an umbrella region. The base of this region is defined by the level of neutral density (height H_B) where the ascending plume has the same density as the surrounding atmosphere. The top of this region (height H_T) is controlled by the momentum of the column at height H_B, which causes the column to rise considerably further than H_B. Typically the ratio $(H_T-H_B)/H_T$ is 0.25 to over 0.3 (see Morton et al. 1956; Sparks 1986). Under steady conditions little further entrainment of air can occur above H_B but continuity demands that the cloud flows sideways in radial fashion. The average radial velocity is defined as:

$$V_R = \frac{M}{2\pi R \alpha (H_T - H_B)}, \quad (2)$$

where M is the mass flow rate of air and ejecta at height H_B, and α is the mean density of air between H_T and H_B. Sparks (1986) found that this simple treatment of the motion in the umbrella region agreed well with the Mount St Helens cloud.

Clasts entering the umbrella region will be transported laterally by the flow. In large columns the velocities can be large and the lateral transport substantial. The maximum range of a clast of given size and density is determined by the motions in this region.

Clast support isopleths

With appropriate expressions for the variation of the vertical velocity with height and radial distance (Eq. 1), contours of constant velocity for eruption columns from H_B=5 km to H_B=30 km at intervals of 5 km have been calculated. The details can be found in Sparks (1986). An example of the velocity distribution is shown in Fig. 2a for H_B=10 km.

At any position in the column there will be clasts which have a terminal fall velocity exactly equal to the ascent velocity. The terminal fall velocity for a clast of diameter d at high Reynolds number is calculated from the following

formula:

$$U_t = C_d \sqrt{\frac{dg\sigma}{\beta}} \quad (3)$$

where Cd is the drag coefficient, σ is the clast density, β is the density of surrounding gas, and 9 is the acceleration due to gravity. In the calculations it is adequate to take Cd=1.054, which is representative of experimental determinations (Wilson 1972; Wilson and Huang 1979). By comparing these fall velocities with the vertical velocity field of the column, envelopes of clast support were constructed. An example is given in Fig. 2b for H_B=10 km for lithic clasts with a density of 2500 kg/m^3. Within an envelope for a particular clast size and density, the terminal velocity is less than the ascent velocity so that the clast is entrained. Outside the envelope the fall velocity exceeds the ascent velocity and the clast will fall out. The clast support surfaces cross-cut the surfaces of constant velocity since the terminal velocities are related to fluid density, which varies with height along a particular velocity surface. Figures 3 and 4 show the same construction for columns with H_B=5, 15, 20, 25 and 30 km.

The geometry of the envelopes has an important control on the fallout of ejecta. In the convective part of the column the sides of the envelope converge downwards enclosing a region with the shape of an inverted cone. Any clast leaving the inner region of entrainment will (in the statistical sense) fall down into regions of decreasing upward velocity and thus fall out completely. However, clasts with trajectories within the envelope can reach into the upper umbrella region. Here the envelope closes and there is a maximum height at which a given clast can be supported. However, clasts will fall back into the region of support unless they leave the envelope at the corner where the region of support has its maximum width. Inspection of Figs. 3 and 4 shows that the maximum width of the support envelope increases substantially as column height increases. It is this width which is the major factor in determining maximum clast size in the fall deposit.

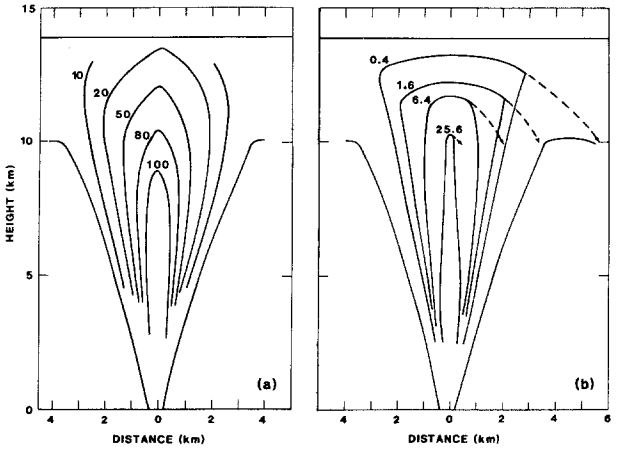

Fig. 2. Velocity variations within an eruption column of H_B=10 km and H_T=13.8 km expressed as (**a**) envelopes of equal velocity in m/s and (**b**) envelopes of particle support where the local upward velocity is just equal to the terminal settling velocities of clasts with diameters of 0.4, 1.6, 6.4 and 25.6 cm and a density of 2500 kg/m^3.

Trajectories in the umbrella region

A clast that reaches the point of maximum width of its support envelope will fall out but will also be swept sideways by the radial velocities caused by expansion of the umbrella region. Figure 5 schematically shows the velocity components that influence a clast trajectory. The vertical velocity decreases in an approximately linear fashion from a maximum value at H_B to zero at H_T along the centreline. Calculations of how the velocity at H_B varies with mass discharge rate can be found in Sparks (1986). This vertical velocity decreases according to the gaussian function away from the centreline. The fall velocity of the clast is its terminal velocity minus the local vertical velocity. A radial (horizontal) velocity component decays as 1/R. This radial velocity is assumed to be independent of height, although velocities probably decrease towards the upper and lower margins of the umbrella cloud. Trajectories have been calculated numerically for an atmosphere with variable air density with height. Once the clast reaches height H_B the fall is approximately vertical to the ground, under the no-wind condition. An inward air flow must occur towards the plume due to entrainment. Even at the plume edge this velocity is only one-tenth of the vertical plume velocity and falls off as the reciprocal of radial distance. This effect is minor and has been neglected.

Figure 6 compares trajectories for 0.4, 1.6 and 6.4 cm lithic clasts (ϱ =2500 kg/m^3) in columns with H_B=15 and 25 km. The calculations show the maximum range of each clast, which is largely determined by the width of its support envelope and the additional transport due to the expanding umbrella region. Figure 6 illustrates the major influence of column height on maximum clast range.

From these calculations a theoretical plot of maximum clast size versus the area enclosed by its isopleth in the fall deposit can be constructed. This is a plot which is commonly used for displaying field data (Walker 1981). Figure 7 shows the theoretical plots for clasts of densities 2500, 1500, 1000 and 500 kg/m^3. The main feature of the diagrams is how sensitive the position of the lines are to column height.

Application to Fogo A

The Fogo A plinian of Saõ Miguel in the Azores is unusual among large plinian fall deposits since the isopachs are circular and the wind must have been weak. The deposit has been documented by Walker and Croasdale (1971). The isopleth contours of maximum pumice and lithic diameters

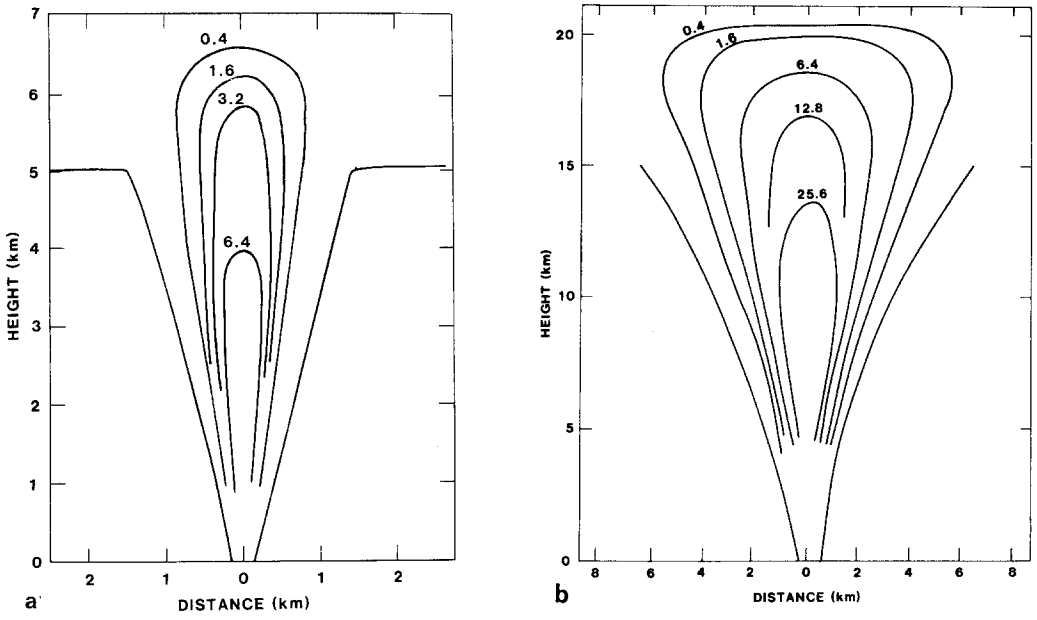

Fig. 3a and b. **a** Clast support envelopes for an eruption column of H_B=5 km and H_T=6.8 km. Envelopes are contoured in terms of clast diameter in centimetres for a density of 2500 kg/m^3. **b** Clast support envelopes for an eruption column of H_B=15 km and H_T=21 km

are almost symmetrical around the vent. The deposit can thus be used to test the model.

Before comparing the field data and theory a digression is necessary on the methods used to collect maximum size data. Unfortunately, different workers have adopted a variety of ways of collecting and analysing maximum clast data. Walker and Croasdale (1971) present the average length of the three largest clasts observed at each outcrop. Many recent studies use the five largest clasts. Japanese workers (Suzuki et al. 1973) measure the ten largest clasts within one square metre. Practice also differs between those who measure clasts *in situ* and those who extract clasts before measuring them.

Walker and Croasdale (1971) sketch in contours which enclose the maximum value found in a number of outcrops. Thus an anomalously large value will determine the position of their contours rather than a statistical average of results at comparable radial distances from the vent. The data of Walker and Croasdale (1971) has been re-analysed by taking the average of all maximum size determinations in concentric zones around the vent. This procedure produces contours which enclose considerably smaller areas for a given size than the contours published by Walker and Croasdale (1971). This treatment is not necessarily better, but the discussion illustrates how the results of applying the model will be somewhat dependent on how the field data are collected and analysed. The data treated in these two different ways are plotted on Fig. 7.

The data plots on two curves which closely parallel the theoretical trends and give confidence that the model is a good approximation of natural behaviour. The lithic data suggest a column of 35 km height, H_T, using the Walker and Croasdale contours and 30 km height using our method of treating the data. If the Fogo A trachytic magma had a temperature of 800 °C these heights are equivalent to magma discharge rates of 1.7×10^8 kg/s (70 000 m^3/s) and 1.0×10^8 kg/s (40 000 m^3/s). Walker (1981) estimated a total volume of deposit of 5.4 km^3 (1.75 km^3 DRE, dense rock equivalent), indicating a total eruption duration of between 6.9-12.1 h. The actual eruption could in fact have been somewhat longer and the average discharge rate lower. Maximum clast data is likely to represent material that falls out at any one locality at the peak discharge (maximum column height). Knowledge of how maximum clast size varied in one locality (and with time) would be required to further refine the estimates.

For large lithic clasts (greater than 10 cm) the two trends depart from the theoretical curve. A plot of maximum lithic diameter versus distance shows a pronounced inflexion in proximal regions (Walker and Croasdale 1971) for large lithics, which they attribute to the influence of clasts emplaced along ballistic trajectories. The present treatment supports their view and confirms that the model will not be relevant to lithic clasts which exceed 10 cm diameter.

The pumice data (Fig. 7) suggest a slightly lower column. However, the pumice may have been denser than 500 kg/m^3 or may have fragmented on impact, as is commonly observed (Sparks et al. 1981), reducing maximum size somewhat. Variable density and impact breakage would make determinations of column height less re-

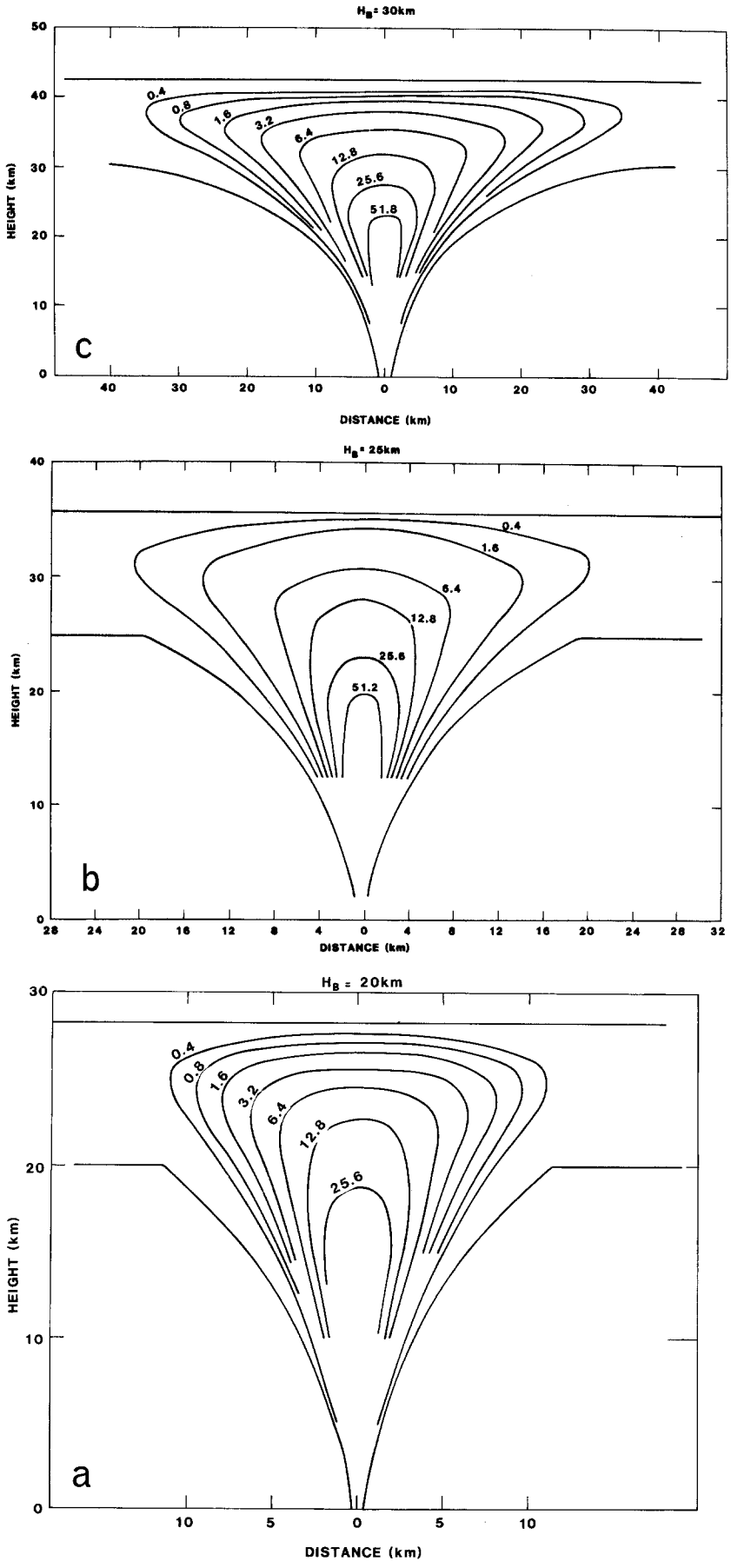

Fig. 4a-c. **a** Clast support envelopes for an eruption column of H_B=20 km and H_T=28.0 km. **b** Clast support envelopes for an eruption column of H_B=25 km and H_T=35 km. **c** Clast support envelopes for an eruption column of H_B=30 km and H_T=43 km

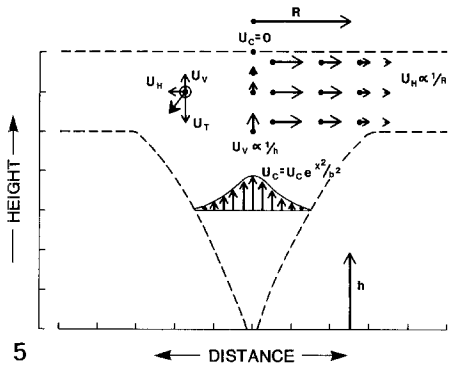

5

Fig. 5. Schematic representation of vertical and horizontal velocity components within an eruption column emplaced in a stably stratified environment. Below H_B the vertical velocity distribution across the plumes is gaussian. Between H_T and H_B the horizontal velocities result from the radial spreading of material passing through the level of H_B. The resultant velocity of a clast falling in the umbrella region consists of the radial velocity (U_H), the partial settling velocity (U_T) and the local vertical velocity (U_V)

liable. If pumice data are used the densities should also be determined and localities where pumice breakage is evident should be eliminated from the data set.

The influence of wind

Axial displacement

Pyroclastic fall deposits typically show isopach and isopleth patterns which are asymmetrical about the source vent, indicating that transport has been influenced by wind. Many theoretical and experimental studies have considered the general problem of buoyant plumes rising in a uniform crossflow (see Briggs 1969). A crossflow will produce several different effects which could influence the characteristics of the resultant fall deposit. The most obvious effect is a bending over of the plume axis in the downwind direction, as is commonly observed for plumes discharged from industrial stacks.

Many theories and empirical formulae have been presented to describe the trajectory of a plume axis and most are variations of the downwind distance raised to the 2/3 power as first suggested by Scorer (1959). Laboratory experiments on buoyant jets and observations on low strength plumes from industrial stacks show good agreement with these relationships (Hoult et al. 1969; Fay et al. 1970; Hoult and Weil 1972; Wright 1977). Their application to volcanic eruption plumes is, however, complicated by several factors. First, the buoyancy fluxes of volcanic eruptions are several orders of magnitude larger than industrial plumes, which rarely exceed 100 MW. Industrial plumes are quickly bent over and a number of simplifications can be made. The commonly cited 2/3 power law is based on an entrainment theory which assumes that the horizontal component of the plume trajectory is equal to the crosswind velocity and that the angles between the plume centreline and horizontal is small. Neither of these assumptions is good for any but the weakest of eruption columns. For these reasons the application of the industrial work to eruption columns must be suspect (Settle 1978; Fedotov 1985).

Another complicating factor is that all of the equations are derived for a uniform crosswind velocity. Because most volcanic eruption plumes transect a large part of the troposphere, and many ponetrate into the stratosphere, they can encounter large variations in horizontal wind speed. This results in shear, for which no set of equations related to plume trajectory has yet been developed.

Lack of any theory for vigorous plumes and the qualitative nature of current observations led us to use a simple model based on the arguments of Wright (1977) that the rise of a vigorous buoyant plume in a crossflow will be similar to that in a stagnant ambient fluid but advected at the velocity of the crossflow. The trajectory of the plume axis is thus calculated by the vector sum of the centreline velocity for a plume with no wind and the wind velocity at that height. Figure 8 shows the results of calculations assuming different wind speeds and column heights. The centreline velocities are those calculated by Sparks (1986), and the maximum wind speed occurs at the temperate

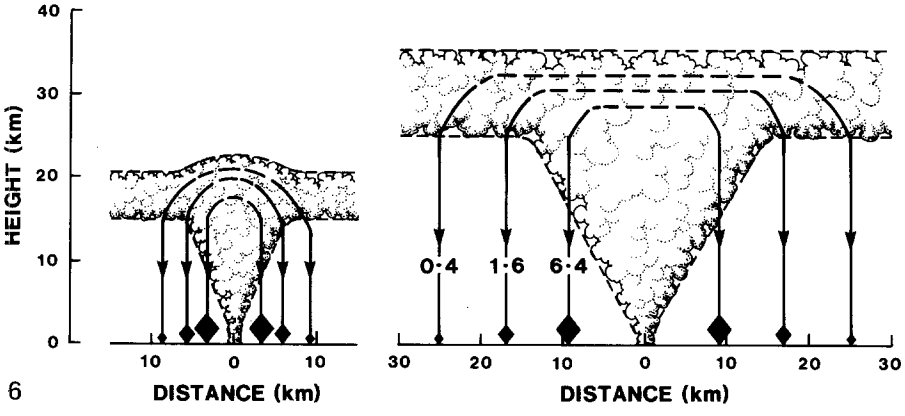

6

Fig. 6. Clast trajectories from the umbrella region to the ground for eruption columns with H_T equal to 21 and 35 km. Note the significant increase in the maximum dispersal of particles for the higher eruption column

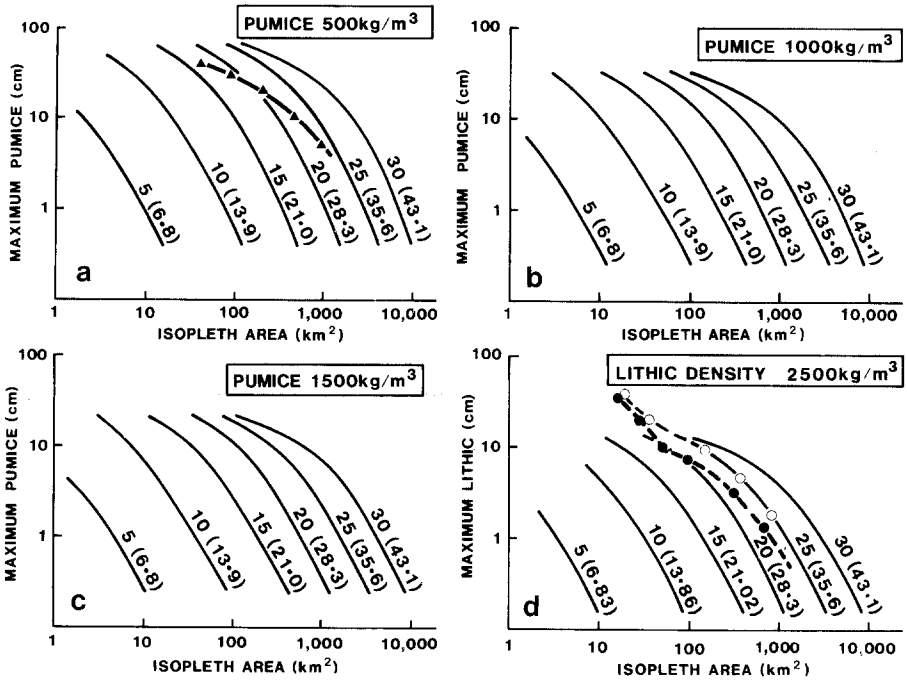

Fig. 7a-d. Isopleth area versus clast size for eruption column heights between 7 and 43 km with clast densities of **a** 500 kg/m^3, **b** 1000 kg/m^3, **c** 1500 kg/m^3 and **d** 2500 kg/m^3. Solid triangles in **a** are pumice isopleths from the Fogo A deposit. Open circles on **d** are lithic field data of the Fogo A pumice-fall from Walker and Croasdale (1971) and solid circles are data of Walker and Croasdale (1971) re-interpreted for the placement of isopleths as described in the text. Values along curves correspond to H_B and H_T (in parentheses) in km

tropopause. The calculations are made up to the height H_B since the influence of the wind in the umbrella region will be treated separately. The calculations show that the axial displacement of the column is small for most columns, although the effect of strong crosswinds on small columns ($H_B < 10$ km) could become significant.

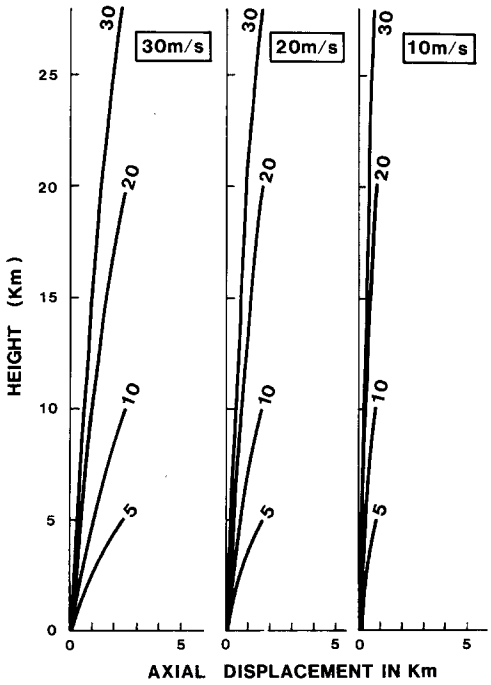

Fig. 8. Axial displacement of eruption columns with H_B=5, 10, 20 and 30 km in crosswinds of 30, 20 and 10 m/s. Displacements are calculated assuming simple advection of the plume at the crosswind velocity

The stagnation point

Observations of the giant cloud of Mount St. Helens on May 18, 1980 allowed an evaluation of the effect of stratospheric winds on a large column (Sparks et al. 1986). The giant cloud expanded radially in accordance with Eq. (2) and reached a stagnation point where the radial expansion velocity was equal to the stratospheric wind velocity. The upwind edge of the cloud then maintained a fixed position. The straightforward behaviour suggests that a very simple treatment of the influence of wind on flow in the umbrella region will be adequate.

In a crosswind, the displacement of the central plume axis at height H_B is calculated as in Fig. 8. Above H_B the flow expands in all directions at velocities determined by the mass flux and radius (Eq. 2). In the upwind direction a stagnation point is reached defining a stationary edge to the umbrella region. A useful measure of the overall plume shape in a crosswind is the ratio of the upwind stagnation radius to the displacement of the plume axis at H_B. Figure 9 shows calculations of the relationship between this ratio and column height for different wind velocities. Sketches of the expected shapes of columns for different values of this ratio are shown. For very large, powerful columns the ratio is much greater than unity, upwind flow in the umbrella region is considerable and axial displacement is limited due to the large convective velocities. The column will be mushroom shaped with a pronounced upwind protrusion (Fig. 10a). For very weak columns, where the ratio is less than unity the wind has a major influence and the column is bent over (Fig. 10c). No true umbrella region forms and a treatment such as those used for industrial plumes may be

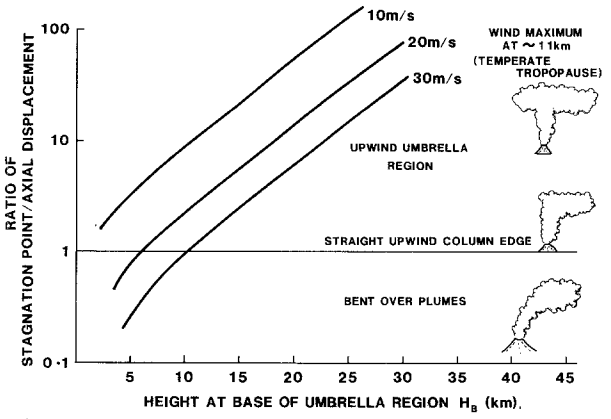

Fig. 9. Ratio of upwind stagnation point to the amount of axial displacement at H_B plotted versus height at H_B for wind speeds of 10, 20 and 30 m/s. Eruptions with ratio >1 produce mushroomed-shaped clouds. At ratio=1 the upwind column edge will be close to vertical whereas at ratio <1 eruption plumes will be significantly bent over

more appropriate than that used here. In plumes with ratio equal to unity we anticipate that the upwind edge of the plume will be vertical (Fig. 10b). In general, columns that are powerful enough to reach the tropopause (10-17 km altitude depending on latitude) will have a ratio greater than unity and will not be significantly bent over. These conclusions seem to be consistent with observations as illustrated by the examples shown in Fig. 10. Fedotov (1985) has come to similar conclusions in his analysis of the effect of wind on volcanic plumes.

Clast trajectories in a crosswind

The procedures used to calculate clast distribution with no wind have been modified to account for the presence of a crosswind. The eruption plume is assumed to rise to its level of neutral buoyancy (H_B) and spread out laterally between H_B and H_T as a forced intrusion. In the presence of a

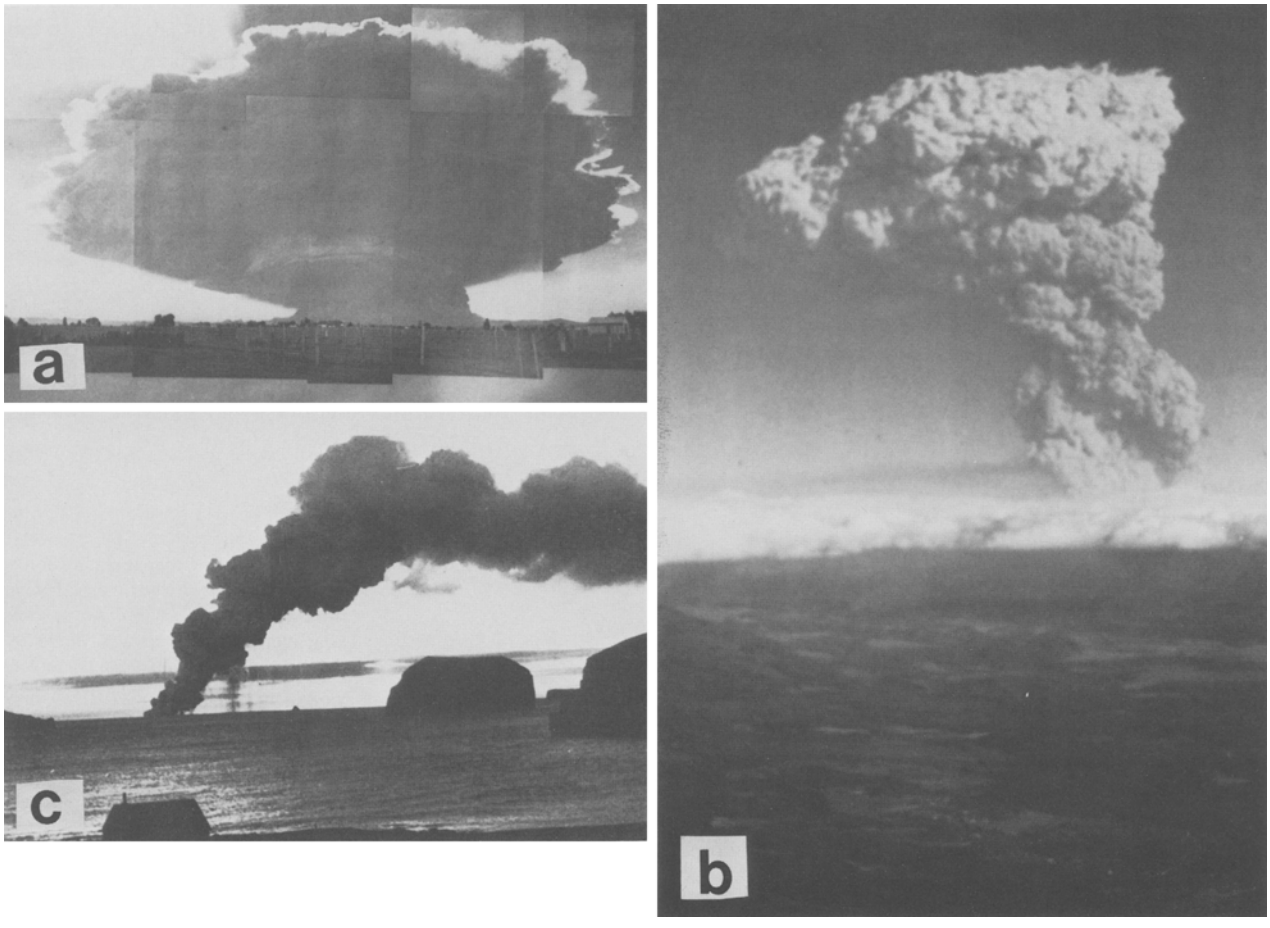

Fig. 10a-c. Shapes of eruption columns. **a** Umbrella shaped giant cloud of Mount St Helens on May 18, 1980. **b** Eruption column of Mount St Helens, 1980. The column is about 14 km high and has a nearly vertical upwind side corresponding to a ratio of 1.0 (see Fig. 9). **c** Eruption column of Surtsey (1963-1967) showing marked axial displacement by wind

crossflow, however, the plume spreads upwind until it reaches a stagnation point where the radial velocity is just equal to the crosswind velocity. A flow pattern is set up whereby the mass flux entering the level at H_B must be conserved through a downwind section normal to the direction of crossflow (Fig. 11). The average velocity through this section is given by

$$V_m = \frac{M}{2\bar{\varrho}\ R_w\,(H_T - H_B)} \tag{4}$$

where V_m is the average flow velocity, M is the mass flux, R_w is the radius of plume spreading normal to the crossflow, $\bar{\varrho}$ is the average plume density between heights H_B and H_T. The radius of plume spreading, R_W, has been determined empirically from the Mount St Helens satellite photographs to be

$$R_w \cong 1.5\,R_s, \tag{5}$$

where R_s is the radius of upwind stagnation. The universality of this relationship is uncertain, but unfortunately this is the only event where the geometry of the cloud has been accurately determined in a known wind-field.

Along a plane normal to the crossflow and cutting through the source, the downwind velocity component due to the deflection of radial expansion by crossflow will be $\frac{1}{2}$ V_m if it is assumed that half of the total mass flux of air and clasts is discharged into the upwind section of the umbrella region. Thus, between this plane and the downwind plane (Fig. 11) the mean velocity must increase from $\frac{1}{2}V_m$ to V_m. The trajectories of clasts leaving the clast support envelope were calculated from three key positions directly upwind of the source, at a radial position normal to the crossflow and at a point directly downwind of the source (Fig. 11). Bending of the plume axis is taken into account by calculating the amount of axial displacement at H_B, assuming that the plume axis is advected at the crosswind velocity, and then shifting the centre of the support envelope symmetry by that amount. No distortion of the clast support envelopes is allowed for, although it must occur at small clast sizes.

In the umbrella region, the trajectory of the side clast has two velocity components: the radial velocity dictated by the forced injection between H_T and H_B and a downwind velocity set up by the establishment of a downwind plume in the crossflow. The upwind clast has a radially imposed velocity which is reduced by the magnitude of the crosswind velocity. At the downwind side of the column, the rear clast follows a trajectory governed by the radial velocity. Below the umbrella region, each of the clasts falls through the atmospheric wind-field. A vertical wind profile similar to that of Shaw et al. (1974) has been adopted. A velocity maximum (varying in steps from 5-30 m/s) occurs at 11 km, or close to the temperate tropopause. The velocity decays in a linear fashion to zero at the ground surface and trends to a constant value of 0.75 of the tropopause maximum in the stratosphere (Fig. 11). In the applications given below a simple wind velocity is cited for each eruption which represents the *maximum* velocity at the tropopause. The calculation procedure follows Carey and Sigurdsson (1982), with the exception that the settling velocity of the clasts is continually adjusted for the variation in atmospheric density. The final locations of the three clasts are used to construct the isopleths of maximum clast size.

Clast trajectories from plumes in crosswinds

Results of numerical calculations for column heights, H_T, of 43, 28 and 13 km with maximum crosswind velocities at the tropopause ranging from 30-10 m/s are shown in Figs. 12-14. Distinct differences can be seen in the geometry of isopleths from various column heights. Large columns

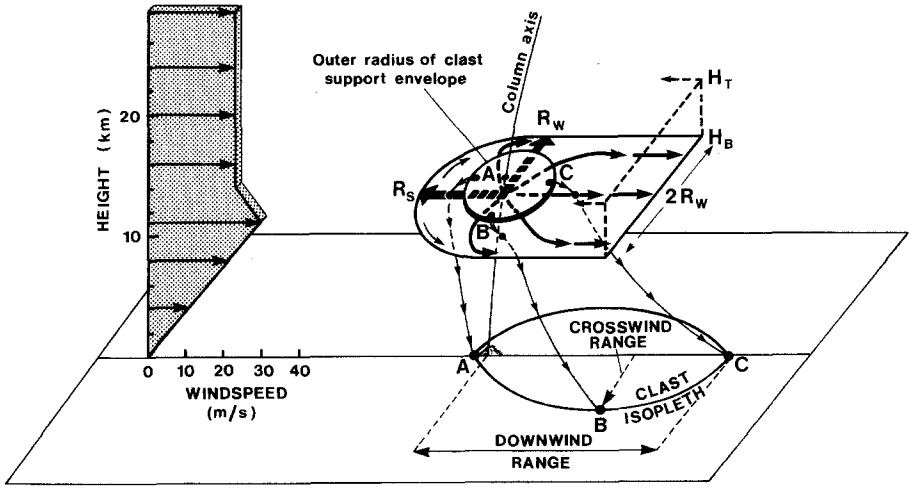

Fig. 11. Schematic representation of the influence of a crosswind on clast fallout from an eruption column. An upwind stagnation point develops at R_s where the radial velocity in the umbrella region equals the crosswind velocity. Radial flow is deflected by the crosswind and passes through the downwind plane defined by H_T, H_B and 2 times R_w (width of radial expansion). Trajectories of three clasts: A (upwind), B (side) and C (downwind) define the geometry of the isopleth measured on the ground. Vertical wind profile adopted for the calculations is shown to the left. Clasts A, B, and C are released from the outer radius of a clast support envelope which lies between the two horizontal planes H_T and H_B

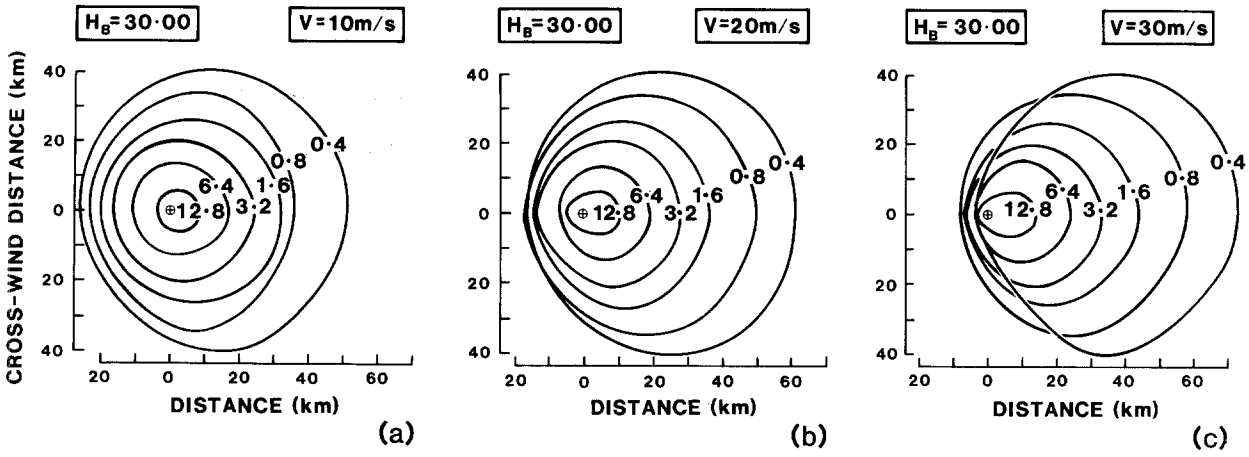

Fig. 12. a Geometry of clast isopleths from an eruption column of 43 km height with a maximum crosswind velocity at the tropopause of 10 m/s. Isopleth contours are for clast diameters in centimetres with a density of 2500 kg/m^3. **b** Geometry of clast isopleths from an eruption column of 43 km height with a maximum crosswind velocity of 20 m/s. **c** Geometry of clast isopleths from an eruption column of 43 km height with a maximum crosswind velocity of 30 m/s. Note the high degree of circular symmetry retained even at high wind speeds

produce isopleths that have a high degree of circularity even with crosswinds of 30 m/s[1]. This is principally the result of most lateral transport occurring by intrusion of material between H_T and H_B. As the column height decreases the ratio of transport within the umbrella region to the transport within the atmospheric wind-field decreases. When the amount of transport in the atmosphere becomes large relative to the expansion in the umbrella region, as is the case for low eruption columns with fast crosswinds, then the isopleths become substantially elongate in the downwind

[1]The reader is reminded that the crosswind velocities referred to are the maximum value on wind profiles with the shape depicted in Fig. 11

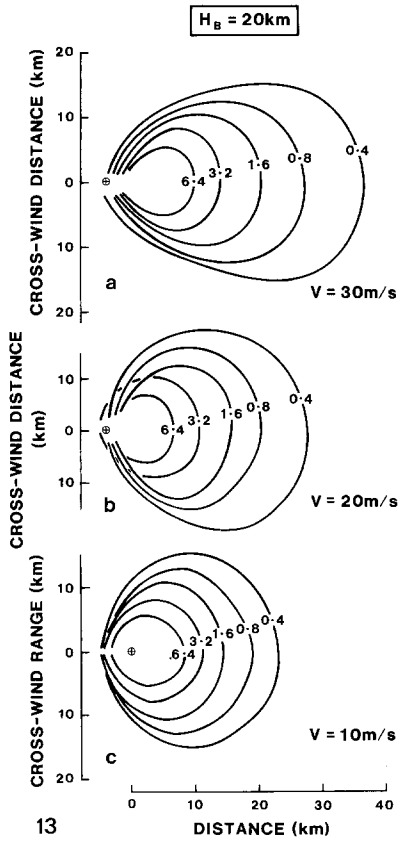

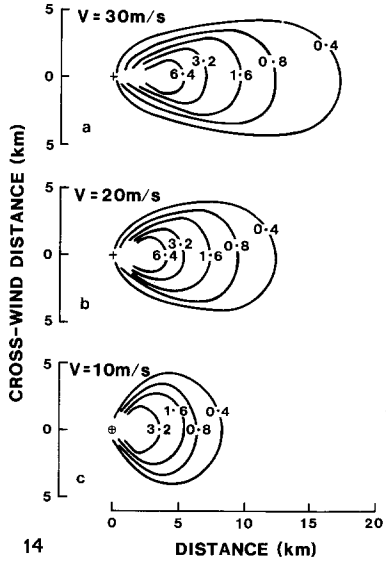

Fig. 13a-c. Isopleth macimum clast patterns for a 28 km high eruption column with maximum crosswinds at the tropopause of **a** 30 m/s, **b** 20 m/s, **c** 10 m/s. Isopleth contours are for clast diameters with a density of 2500 kg/m^3

Fig. 14a-c. Isopleth maximum clast patterns for a 14 km high eruption column with maximum crosswinds at the tropopause of **a** 30 m/s, **b** 20 m/s, **c** 10 m/s

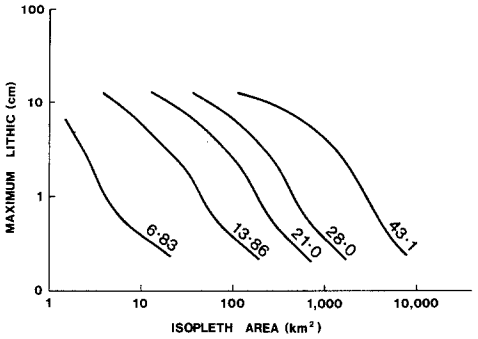

Fig. 15. Isopleth area versus clast size for eruption columns between 7 and 43 km with a maximum crosswind at the tropopause of 30 m/s. Isopleth areas in crosswinds are increased relative to the no-wind conditions (Fig. 7). Clast density equals 2500 kg/m^3

direction and take on a characteristically ellipsoidal shape (Fig. 14a).

The effect of a crosswind is to increase the area enclosed by a given isopleth but, as one might expect from the above arguments, the magnitude of the area increase is larger for small eruption columns and small for larger columns. This can be seen by comparing Fig. 7 with Fig. 15, which gives the isopleth areas for a maximum crosswind of 30 m/s and a range of column heights from 6.8-43 km.

Because the width of an isopleth perpendicular to the crosswind is principally a function of the column height, and the maximum downwind range is a function of both the column height and the wind speed, diagrams can be constructed that allow discrimination of the two effects based on the geometry of a given isopleth. Figure 16 shows plots of the crosswind radius versus the maximum downwind range for theoretical isopleths of clast sizes 0.8, 1.6, 3.2 and 6.4 cm in diameter. The two parameters can be seen to define uniquely the column height and wind speed for a particular isopleth geometry. It must be stressed, however, that these diagrams portray combinations dependent upon the assumed wind profiles. Although the effect of column height, i. e. crosswind radius, will remain unchanged, the position of the isowindspeed curves will adjust according to whatever vertical profile is adopted. The profile used in these calculations (see Fig. 11) is a reasonable estimate of the types of wind systems many eruptions are likely to encounter in temperate latitudes. Instead of modelling all the likely configurations of wind profiles at different latitudes, copies of the program can be supplied to those interested in modelling specific cases with instructions as to how to modify the program to any type of wind profile.

Another factor which may influence calculations is variation in wind direction, which will increase the apparent cross wind range and thus overestimate column height. Winds in the stratosphere tend to remain fixed in direction for periods comparable to or greater than most plinian eruptions. Thus in short-lived high intensity eruptions this effect is likely to be small. However, long-lived weak eruptions, such as strombolian events, could last for weeks or months and low-level winds may vary considerably in direction. In these circumstances cross wind distance may be impossible to measure or would be overestimated.

Application of the crosswind model

In this section the results of the theoretical model are compared with field data. Two historic eruptions are considered first, for which estimates of at least column height, and in one case wind speed, are available. These eruptions, the 1902 plinian eruption of Santa Maria volcano in Guatemala (Williams and Self 1983) and the May 18, 1980 eruption of Mount St. Helens (Waitt and Dzurisin 1981; Carey and Sigurdsson 1982), will provide important tests for the accuracy of the model. The column heights given are the height H_T and the wind velocities refer to the maximum velocity at the tropopause as depicted in the profile in Fig. 11. Calculated and observed heights and wind velocities are compared in Table 1.

Mount St. Helens (May 18, 1980)

Limited pumice isopleth data is available for the plinian phase of the May 18, 1980 eruption of Mount St. Helens (Waitt and Dzurisin 1981); unfortunately no mention is made as to the nature of the measurements (average of 3, 5, 10 fragments?). The data are sufficient to test two clast sizes, 4 and 8 cm diameter, which are the hydraulic equivalents of 0.8 and 1.6 cm lithics (Fig. 16). From these two isopleths, the average column height and wind speed based on our model are 19 km and 36 m/s respectively. Radar measurements of the eruption column height during the May 18 event show a peak of 19 km at 1700 hours Pacific Zone time (Harris et al. 1981) and a maximum wind speed between 27 and 33 m/s was measured by radiosonde near the tropopause (Danielsen 1981; Carey and Sigurdsson 1982). The results of the model thus agree quite well with radar and meterorological observations in spite of the uncertainties in the field data. The proximal plinian deposit is reversely graded and the published maximum grain size only allows conditions at the peak intensity to be inferred. The average height of the column was 16 km.

Santa Maria (October 25, 1902)

The plinian eruption of Santa Maria volcano, Guatemala on October 25, 1902 discharged at least 8.5 km^3 of dacitic magma (DRE) and was one of the largest explosive eruptions of this century (Williams and Self 1983). Based on the model a column height of 34 km and a windspeed of 14 m/s are estimated (Fig. 16). During the course of the eruption two sets of measurements were made of the column height. One, by the mailboat S. S. *Newport*, reported the height to be between 27 and 29 km, whereas a second estimate placed the height at 48 km (Anderson 1908). Williams and Self (1983) calculated the column height independently using

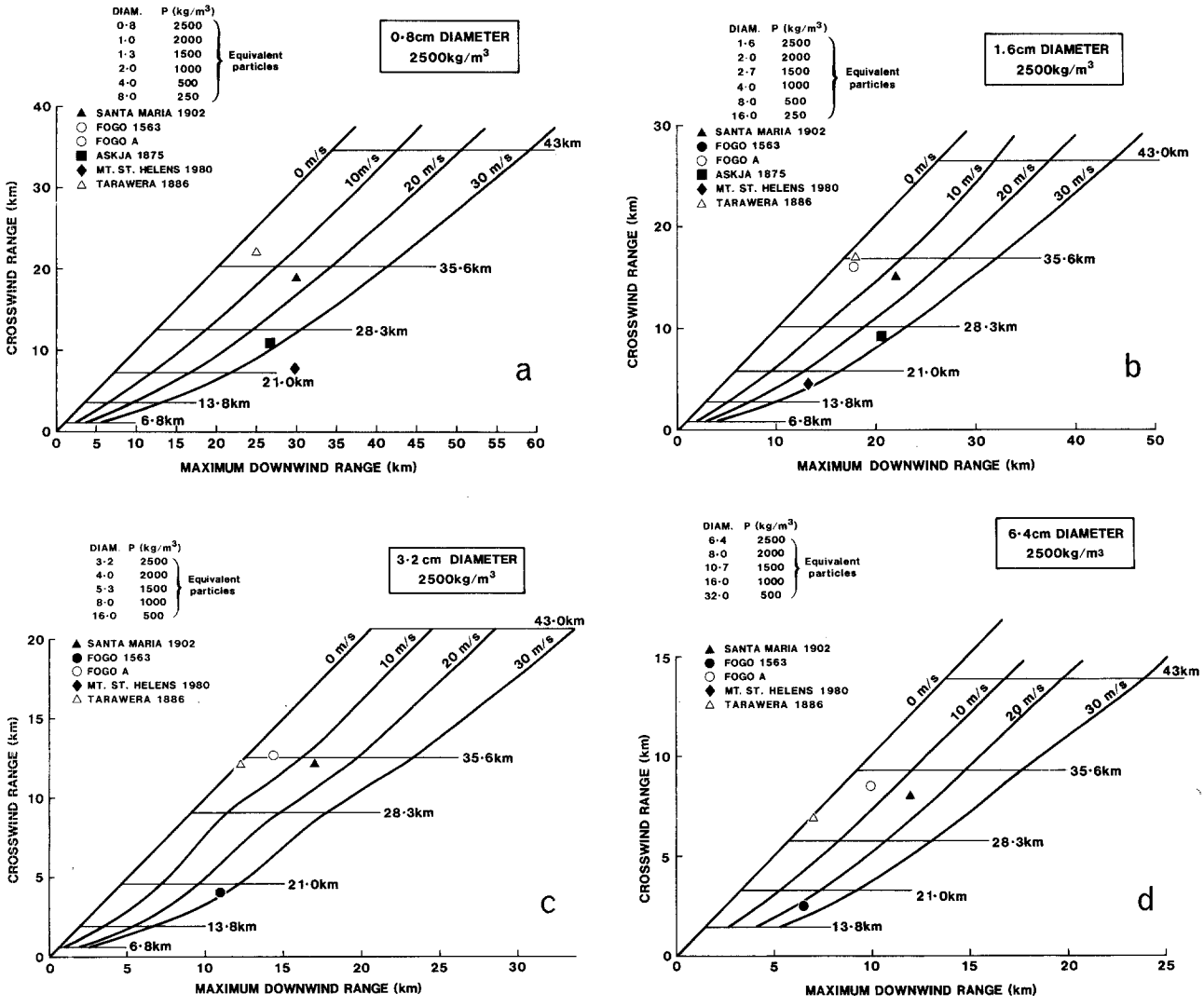

Fig. 16. **a** Crosswind range versus maximum downwind range for 0.8 cm diameter clasts with a density of 2500 kg/m^3 from eruption columns between 7 and 43 km with wind speeds of 10, 20 and 30 m/s. **b** Crosswind range versus maximum downwind range for 1.6 cm diameter clast isopleths from eruption columns between 7 and 43 km with wind speeds of 10, 20 and 30 m/s. **c** Crosswind range versus maximum downwind range for 3.2 cm diameter clast isopleths from eruption columns between 7 and 43 km with wind speeds of 10, 20 and 30 m/s. **d** Crosswind range versus maximum downwind range for 6.4 cm diameter clast isopleths from eruption columns between 7 and 43 km with windspeeds of 10, 20, 30 m/s. A single clast isopleth defines a unique combination of clumn height and wind speed. Data from several explosive eruptions are plotted and can be discriminated by the key. A list of lower density clasts which are hydraulically equivalent to a 0.8 cm lithic is shown

the plume rise equation of Wilson et al. (1978) and volume of magma determined by their fieldwork. Their calculated height of 35 km is in good agreement with our prediction and is consistent with the visual observations of column height on October 25.

These two examples of historic eruptions, for which column height and wind speed are known with some degree of certainty, demonstrate a good correspondence between observed and predicted values. Additional applications of the model are now presented for eruptions where a lesser degree of cross-checking is possible.

Askja

The 1875 explosive eruption of Askja, Iceland included a plinian phase which lasted about 6.5 h (Sparks et al. 1981). Activation and eruption of a rhyolitic magma body beneath the Askja central volcano was apparently triggered by influx of ferrobasaltic magma that both mixed with the rhyolite and flowed laterally along a fissure swarm to the Sveinagja area (Sigurdsson and Sparks 1978). Following an initial phreatoplinian phase, the main plinian eruption produced a coarse, widespread, reversely-graded fall

Table 1. Column heights and wind speeds for several explosive eruptions

Eruption	Predicted[a]		Observed		No. of isopleths
	col. ht. (km)	wind speed (m/s)	col. ht.	wind speed	
Mount St Helens May 18, 1980	19.0	36.0	19.0	33.0	2
Santa Maria October 25, 1902	34.0	14.0	27-48		4
Askja, 1875	26.0	43.0	—	>25	4
Tarawera, 1886	34.0	4.0	—	—	4
Fogo, 1563	18.5	25.0	—	—	2
Taupo	51.0	27.0	—	—	4

[a] Predicted column height and wind speed are the averages of individual determinations from Fig. 16. The number of isopleths included in the average is shown on the right

deposit (unit D, Sparks et al. 1981). The wind velocity is estimated at 25 m/s from data on tephra fallout across the Atlantic and in Scandinavia (Thorarinsson 1963). Maximum grain size data is only available on pumice which was unusually low in density (250 kg/m^3). Thus the hydraulic equivalent of a 1.6 cm lithic is a 16 cm pumice clast. The field data is only reliable for 16 and 8 cm pumice clasts. The wind velocities calculated from clasts of this size are reasonably consistent with observations and a maximum column height of 26 km is estimated (Fig. 16). The high wind speed resulted in the narrow and highly elongated depositional pattern of the Askja fall deposit.

The estimate of column height can be used in conjunction with the known duration of the plinian phase to estimate the volume of ejected rhyolitic magma. A 26 km high column would correspond to a mass eruption rate of 8.2×10^7 kg/s, assuming a magma temperature of 850 °C. If the rate was constant during the 6.5 hour period then 0.83 km^3 (DRE) of magma would have been produced. This is considerably larger than the 0.16 km^3 (DRE) determined by Sparks et al. (1981) for the main plinian phase (unit D) and helps reduce the large discrepancy noted between the observed caldera volume (2.0 km^3) and the original estimate of total magma ejected (0.21 km^3). However, the volume calculated from the inferred mass eruption rate assumes a constant discharge over the entire period. The strong reverse grading in the fall deposit suggests that the intensity of the eruption was increasing with time. Thus the volumes calculated from the constant column height assumption represent the maximum values. A similar overestimate of both discharge rate and duration is apparent when the calculated height of the Mount St Helens column is used.

Tarawera (1886)

The 1886 Tarawera eruption was New Zealand's largest volcanic eruption of historic times (Walker et al. 1984). Discharge of basaltic magma occurred along a 17 km fissure over a period of roughly 4 hours. A widespread scoria-fall was produced which has been interpreted by Walker et al. 1984) as a rare example of a basaltic plinian deposit. However, recent studies by B. F. Houghton and C. J. N. Wilson (personal communication) suggest that a discrete plinian vent cannot be identified and that vigorous activity occurred along the entire length of the fissure.

Walker et al. (1984) suggest that because the eruption cloud was of much greater vertical extent relative to the dimensions of the fissure, the eruption cloud essentially "forgot" its linear source and acted as a point source. Based on the lithic isopleths a column height of 34 km and a wind speed of 4 m/s are estimated (Fig. 16). This is consistent with a mass eruption rate of 1.8×10^8 kg/s, as calculated by Walker et al. (1984), but for a magma temperature of 1050 °C. A somewhat lower column height of 27.8 km cited by Walker et al. (1984) for the same mass eruption rate is apparently the result of either a lower estimate of magma temperature or a lower value of F (the efficiency factor of heat transfer, Wilson et al. 1978).

The relatively low inferred wind speeds ($\sim$4 m/s) are consistent with the general circular symmetry of the isopachs and isopleths of the scoria deposit and the still clear night reported by witnesses (C. J. N. Wilson, pers. comm.). These wind speeds are considerably less than the 15.5 m/s mean wind speeds deduced by Walker et al. (1984) from the fall times and net downwind displacement of a range of particle sizes. The difference can be attributed to the higher eruption column height in the model and the configuration of the adopted wind profile.

Fogo (1563)

Unlike the windless Fogo A eruption, the Fogo 1563 plinian pumice fall exhibits evidence of influence by a strong crosswind. Walker and Croasdale (1971) noted the better sorting in the 1563 deposit compared to the Fogo A and attributed

it to the effect of wind. Lithic isopleths of the deposit indicate an eruption column height of 18.5 km and a wind speed of 25 m/s (Fig. 16). The column height was thus only half that of the Fogo A eruption and the influence of a strong crosswind is confirmed. These results suggest that the Fogo 1563 event was similar in intensity and environmental conditions to the May 18, 1980 eruption of Mount St. Helens.

The volume of the Fogo 1563 deposits is 1.3 km^3 (tephra), or 0.34 km^3 (DRE) assuming a bulk deposit density of 600 kg/m^3 (Walker, 1981). An 18.5 km eruption column discharging magma at 850 °C would have a mass eruption rate of 1.9×10^7 kg/s and a 12.9 hour period would be required to produce the total volume of ejected magma. This duration estimate is supported by the fact that whereas the intensity and dispersal of pyroclasts are similar for the Fogo 1563 and Mount St. Helens eruption (9.5 h), the thickness of the Fogo deposit at a given distance is greater than the Mount St. Helens pumice-fall. Walker (1981) reports a duration of 2 days. The discrepancy between this and the calculation may either reflect a discontinuous eruption or may be due to the original observations recording other activity apart from the plinian event or to the estimated column height representing the maximum rather average conditions.

Taupo (1820 B.P.)

At the extreme end of known plinian fall deposits lies the Taupo plinian pumice of New Zealand, which in fact Walker (1980) has classified separately as ultraplinian based on its extensive dispersal. Lithic isopleths from the Taupo pumice yield a column height of 51 km and a rather strong windspeed of 27 m/s. Walker (1980) suggested that the column height was in excess of 50 km and our results confirm his contention. The total volume of the fall deposit is 23 km^3 (tephra) or 5.8 km^3 (DRE). A column of 51 km height would have a remarkably high mass eruption rate of 1.1×10^9 kg/s yet would only require a duration of 3.8 hours to eject the calculated volume of magma. The deposit is reversely graded and the maximum grain size data of Walker (1980) refers to the coarsest part. Thus the actual duration would have been longer since the earlier parts of the eruption phase must have had lower discharge rates. The inferred column height of 51 km is close to the theoretical limit of 55 km suggested by Wilson et al. (1978), based on an analysis of the stability of convective columns.

Discussion and conclusion

A theoretical model of pyroclast fallout from eruption columns has been developed from the general theory of buoyant plume rise (Morton et al. 1956) modified for volcanic eruptions by Wilson et al. (1978), Sparks and Wilson (1982) and Sparks (1986). The present analysis is concerned only with the maximum dispersal of clasts. Maximum clast size measurements are routinely collected for pyroclastic fall deposits and displayed on maps as maximum clast isopleths. A simple geometrical configuration of the column has been adopted whereby an umbrella region is formed over an expanding column by the forced intrusion of material between the level where the column density is equal to the surrounding atmosphere (H_B) and the maximum height attained as a result of excess momentum (H_T). Within these boundary limits the entrainment and transport of clasts is controlled by the average vertical velocity, which can be portrayed as a series of particle support envelopes where the vertical velocity of the column is equal to the terminal settling velocity of a specific clast size and density. The maximum dispersal of a specific clast size is determined to a large extent by the location of the edges of its mushroom-shaped support envelope, under conditions of no wind. Additional radial transport in the umbrella region is imposed by the lateral intrusion of plume material.

The present models have been developed for magmatic explosive eruptions in which the main driving force comes from decompression of magmatic gasses. In phreatomagmatic eruptions the large quantities of external water and steam probably exert an important influence on the behaviour of eruption columns and dispersal of ejecta. A thorough investigation of wet phreatomagmatic eruption columns has yet to be made and we suggest caution in applying these models to deposits where water is thought to have had a major influence.

The model predicts that, except for the weakest eruptions, fist-sized clasts (5 cm lithics) can be transported into the top of the column. These clasts may not be widely dispersed, however, because of the narrow width of the support envelopes in moderate-sized eruptions. The height and width of the support envelopes are strongly dependent on the eruption column height or the rate at which magma is erupted (Wilson et al. 1978). The area over which a given size clast will fall is thus strongly correlated with column height.

A comparison of predicted isopleths for column heights between 6.8 and 43 km with field data for the Fogo A pumice-fall deposit in the Azores demonstrates a similarity in the trend of isopleth area versus particle size and leads us to conclude that the first order processes are adequately modelled. The Fogo A deposit is a rare example of pyroclast accumulation with negligible effects of a crosswind, and an eruption column height of 30—35 km is inferred.

The effects of crosswinds on eruption columns and clast transport have been investigated. An important feature revealed by satellite observations of the initial Mount St. Helens cloud was the development of a stagnation point in the upwind direction from the source. Wholesale bending of the column axis also occurs in response to a crosswind but, despite the abundance of theories and formulae dealing with this general problem, their application is limited by the very large buoyancy fluxes associated with volcanic erup-

tions and assumptions of constant wind speed. In general, they provide satisfactory predictions for low-level plume trajectories such as industrial gases from stacks and are thus only useful for the weakest of explosive eruptions.

Qualitatively, the shape of eruption columns can be inferred by considering the location of the upwind stagnation point relative to the amount of downwind axial bending that has occurred at the level of H_B. For lack of a proper theory we adopt a "worst-case" displacement calculation that assumes advection of the column axis at the crosswind speed. High altitude columns, by virtue of their large mass flux and relatively small axial displacement are able to spread upwind and evolve into an anvil-shaped cloud with an extensive umbrella region. As column height is decreased, a point is reached where the stagnation radius is roughly equal to the amount of axial displacement and the column will have a nearly vertical upwind side. A good example of this is the plinian column developed over Mount St. Helens on May 18, 1980 following the initial surge and flow activity. For very low columns the amount of axial bending is quite large relative to the amount of upwind spreading, if any, and a bent-over plume resembling the industrial smokestack discharge is produced.

Modelling of pyroclast fallout in a crosswind has been carried out using an upwind stagnation point, axial displacement up to the level of H_B by simple advection at the crosswind velocity, and conservation of mass flow through a downwind plume section. The results demonstrate the relative contributions of column height and wind speed to the geometry of the resulting isopleth. Very high eruption columns produce isopleths that retain a high degree of circular symmetry even with strong crosswinds. Lateral transport of particles within the umbrella region is thus large relative to the residual atmospheric transport below the umbrella. As column height is decreased the amount of atmospheric transport begins to dominate over the lateral spreading in the umbrella region and the isopleth shapes evolve towards a more ellipsoidal geometry. Two parameters of the isopleth shape, the maximum half-width perpendicular to the wind direction and the maximum downwind range from source, can be used to estimate the column height and wind speed for a particular eruption. The inferred wind speed is, of course, dependent on the wind profile chosen for the model, whereas the column height remains largely dependent on the initial assumptions of the column structure and dynamics. The crosswind range can also be increased by changing wind direction and may lead to slight overestimation of column heights in some cases. When applied to two historic eruptions of Mount St. Helens and Santa Maria volcano in Guatemala, the predicted values of column height and wind speed derived from isopleth geometries agree well with actual observations. The model thus provides a new tool which can be used to determine column heights, mass eruption rates and environmental conditions of ancient explosive eruptions.

Acknowledgements. Support for this work was provided by grants from the National Science Foundation (EAR 84-155028, S.N.C.) and the BP Venture Research Unit, (R.S.J.S.). Most of the work was completed during a visit to the Woods Hole Oceanographic Institution by R.S.J.S. and during a visit to the Department of Earth Sciences, Cambridge University, by S.N.C., for which travel funds were provided by NSF. We gratefully acknowledge discussions with Stewart Turner, George Walker, Colin Wilson, Lionel Wilson and Herbert Huppert which contributed to the development of the model. The work owes a great deal to George Walker who has developed the systematic field studies of air-fall deposits which provided the motivation for the theoretical study.

References

Allen JRL (1982) Particle motions at low concentrations: grading in pyroclastic-fall deposits. In: Sedimentary Structures, their character and physical basis, Vol 1 pp 111-134, Elsevier, Amsterdam

Anderson T (1908) The volcanoes of Guatemala. Geogr J 31: 473-489

Brazier S, Davies AN, Sigurdsson H, Sparks RSJ (1982) Fallout and deposition of volcanic ash during the 1979 explosive eruption of the Soufriere of St Vincent. J Volcanol Geothermal Res 14: 335-359

Briggs GA (1969) Plume Rise. US Atomic Energy Commission, pp 1-80

Carey S, Sigurdsson, H (1982) Influence of particle aggregation on deposition of distal tephra from the May 18th, 1980 eruption of Mount St Helens Volcano. J Geophys Res 87: 7061-7072

Carey S, Sigurdsson H (1985) The May 18th, 1980 eruption of Mt St Helens, 2, Modelling of Dynamics of the plinian phase. J Geophys Res 90: 2948-2958

Carey S, Sigurdsson H (1986) The 1982 eruptions of El Chichon Volcano, Mexico (2): Observations and numerical modelling of tephra-fall distribution. Bull Volcanol 48: 127-141

Danielsen E (1981) Trajectories of the Mount St Helens eruption plume. Science 211: 819-821

Eaton GP (1963) Volcanic ash deposits as a guide to atmospheric circulation in the geologic past. J Geophys Res 68: 521-528

Fay J, Escudier M, Hoult D (1970) A correlation of field observations of plume rise. J Air Pollut Control Assoc 20: 391-397

Fedotov, SA (1985) Estimates of heat and pyroclast discharge by volcanic eruptions based upon the eruption cloud and steady plume observations. Geodynamics 3: 275-302

Harris DM, Rose WI, Roe R, Thompson MR (1981) Radar observations of ash eruptions. USGS Prof Pap 1250: 323-334

Hoult D, Fay J, Forney L (1969) A theory of plume rise compared with field observations. J Air Pollut Control Assoc 19: 585-590

Hoult D, Weil J (1972) Turbulent plume in a laminar cross-flow. Atmos Environ 6: 513-531

Knox JB, Short NM (1964) A diagnostic model using ash fall data to determine eruption characteristics and atmospheric conditions during a major volcanic event. Bull Volcanol 27: 5-24

Morton B, Taylor GI, Turner JS (1956) Turbulent gravitational convection from maintained and instantaneous sources. Proc Roy Soc A234: 1-23

Rice CJ (1981) Electro-optical instrumentation for resources evaluation. Proc Intern Soc Optical Engineering 278: 23-31

Rouse H, Yih CS, Humphreys HW (1952) Gravitational convection from a boundary source. Tellus: 201-210

Scorer RS (1959) The behaviour of chimney plumes. Int J Air Pollut 1: 198-220

Settle M (1978) Volcanic eruption clouds and the thermal power output of explosive eruptions. J Volcanol Geotherm Res 3: 309-324

Shaw DM, Watkins ND, Huang TC (1974) Atmospherically transported volcanic glass in deep sea sediments: theoretical considerations. J Geophys Res 79: 3087-3094

Sigurdsson H, Sparks RSJ (1978) Rifting episodes in north Iceland in 1874-75 and the eruption of Askja and Sveinagja. Bull Volcanol 41: 1-19

Slaughter M, Hamil M (1970) Model for deposition of volcanic ash and resulting bentonite. Geol Soc Am Bull 81: 961-968

Sparks RSJ (1986) The dimensions and dynamics of volcanic eruption columns. Bull Volcanol 48: 3-15

Sparks RSJ, Moore JG, Rice CJ (1986) The initial giant umbrella cloud of the May 18th, 1980, explosive eruption of Mount St Helens. J Volcanol Geothermal Res (in press)

Sparks RSJ, Wilson L (1982) Explosive Volcanic Eruptions — V. Observations of plume dynamics during the 1979 Soufriere eruption, St Vincent. Geophys J R Astr Soc 69, 551-570

Sparks RSJ, Wilson L, Sigurdsson H (1981) The pyroclastic deposits of the 1875 eruption of Askja. Phil Trans R Soc Lond 299: 241-273

Suzuki T (1983) A theoretical model for dispersion of tephra. In: D Shimonguru, Yokoyama I (eds) Arc Volcanism: Physics and Tectonics, pp 95-116

Suzuki T, Katsui Y, Nakamura T (1973) Size distribution of the Tarumai T_a-T_b pumice fall deposit. Bull Volcanol Soc Japan 18: 47-63

Thorarinsson S (1963) Askja on Fire. Almenna Bokafelgid, Reykjavik, Iceland

Turner JS (1979) Buoyancy Effects in Fluids. Cambridge University Press pp 1–368

Waitt RB, Dzurisin D (1981) Proximal air-fall deposits from the May 18 eruption: stratigraphy and field sedimentology. USGS Prof Pap 1250: 601-616

Walker GPL (1973) Explosive volcanic eruptions — a new classification scheme. Geol Rudsch 62: 431-446

Walker GPL (1980) The Taupo pumice: product of the most powerful known (ultraplinian) eruption! J Volcanol Geotherm Res 8: 69-94

Walker GPL (1981) Plinian eruptions and their products. Bull Volcanol 44: 223-240

Walker GPL, Croasdale R (1971) Two plinian-type eruptions in the Azores. J Geol Soc London 127: 17-55

Walker GPL, Self S, Wilson L (1984) Tarawera 1886, New Zealand — a basaltic plinian fissure eruption. J Volcanol Geotherm Res 21: 61-78

Walker GPL, Wilson L, Bowell ELG (1971) Explosive Volcanic Eruptions —I: Rate of fall of pyroclasts. Geophys J R Astr Soc 22: 377-383

Williams SN, Self S (1983) The October 1902 plinian eruptions of Santa Maria Volcano, Guatemala. J Volcanol Geotherm Res 16: 33-56

Wilson L (1972) Explosive Volcanic Eruptions — II. The atmospheric trajectories of pyroclasts. Geophys J R Astr Soc 30: 381-392

Wilson L (1976) Explosive Volcanic Eruptions — III. Plinian eruption columns. Geophys J R Astr Soc 45: 543-556

Wilson L (1980) Relationships between pressure, volatile content and ejecta velocity in three types of volcanic explosion. J Volcanol Geotherm Res 8: 297-313

Wilson L, Huang TC (1979) The influence of shape on the atmospheric settling velocity of volcanic ash particles. EPSL 44: 311-324

Wilson L, Sparks RSJ, Huang TC, Watkins ND (1978) The control of volcanic column heights by eruption energetics and dynamics. J Geophys Res 83: 1829-1836

Wilson L, Sparks RSJ, Walker GPL (1980) Explosive Volcanic Eruptions IV. The control of magma properties and conduit geometry on eruption column behaviour. Geophys J R Astr Soc 63: 117-148

Wright SJ (1977) Mean behaviour of buoyant jets in a cross-flow. J Hydraulics Div: ASCE 103: 499-513

Received November 1, 1985 / Accepted January 13, 1986